Journal of New Materials for Electrochemical Systems 18, 193-205 (2015)

Recent Progress in Structural and Electrochemical Properties in Composite Based $LiFePO_4$ Batteries

Lubna Tabassam[1,*], Uzma Tabassam[1,†] and Umair Manzoor[1,2]

[1]Department of Physics, COMSATS Institute of Information Technology, Park Road, Chak Shahzad campus, Islamabad, Pakistan
[2]Alamoudi Water Research Chair, King Saud University, Riyadh. Kingdom of Saudi Arabia

Received: September 02, 2015, Accepted: October 08, 2015, Available online: October 30, 2015

Abstract: *This review describes some recent developments in the composite doped cathode materials such as $LiCoO_2$, $LiNiO_2$, $LiMn_2O_4$, and $LiMnO_2$ with focus on $LiFePO_4$. Olivine $LiFePO_4$ have attracted considerable attention since last decade because of its promising properties as a cathode material in Li ion based batteries (LIBs), that is, it offers high theoretical capacity, environmental friendliness, and less toxicity. The electrochemical and structural characterization of this system will be discussed in more detail as compared with its other counterpart.*

Keywords: Cathode material, Olivine structure, Electrochemical and structural properties

1. INTRODUCTION

Rechargeable Lithium Ion Batteries (LIBs) have become very important components in portable, telecommunication, computers, and entertainment devices required by information-rich systems. LIBs are required in mobile society, such as camcorders, MP4-players, lap tops and cellular phones. The development of improved battery technology is the crucial issue in various applications of hybrid electric vehicles to consumer electronics. Since last 25 years $LiCoO_2$/C has been used extensively as cathode material for this purpose after Sony Corporation first commercialized the composite in 1991. This class of material is found almost in every battery driven gadget – presently being manufactured at a rate of several millions of units per month. The rechargeable LIBs have an operating potential over 3.6 V, which is three times higher than that of alkaline systems. In addition, the energy densities of LIBs are as high as 120–150 W h kg^{-1}, which is two or three times larger than those of Ni–Cd batteries [1].

A lithium ion battery is an electrochemical cell that transforms chemical energy into the electric energy, see Figure 1. The key components of LIB are a) anode, b) cathode and c) electrolyte. For the commercialization of LIB system, both cathode and anode materials are intercalation materials - the anode made up of graphite and cathode made up of transition metal oxides, such as. Li(Co, Ni, Mn)O_2. In charging process, Li ions are extracted from the cathode, moved through the non-aqueous electrolyte and intercalated into the anode. While in discharge process, all the Li ions are moved back to the cathode sides and the process is vice versa. Meanwhile, electrons also move from cathode to anode through the outside current collectors forming an electric circuit. The chemical potential of Li is much higher in anode than in the cathode, thus the electric energy is stored in the form of chemical energy [2]. The cathode and anode region are separated by the separator. A separator is a very thin sheet of (polymer) micro-porous

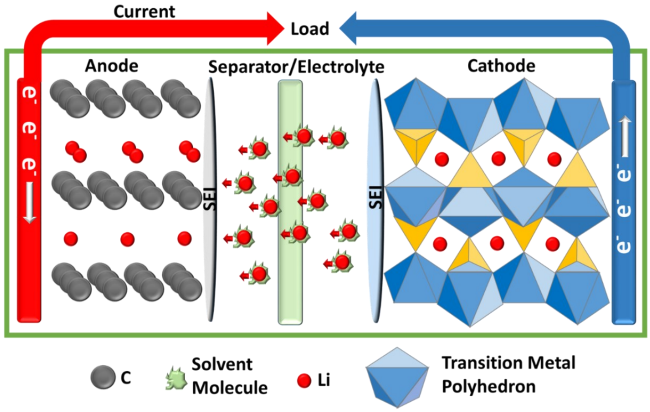

Figure 1. Working principle of lithium ion battery (charging).

To whom correspondence should be addressed:
Email: *lubna.tabassam@comsats.edu.pk; †uzma.tabassam@comsats.edu.pk
Phone: +92-51-3335529948; +92-51-3359145354

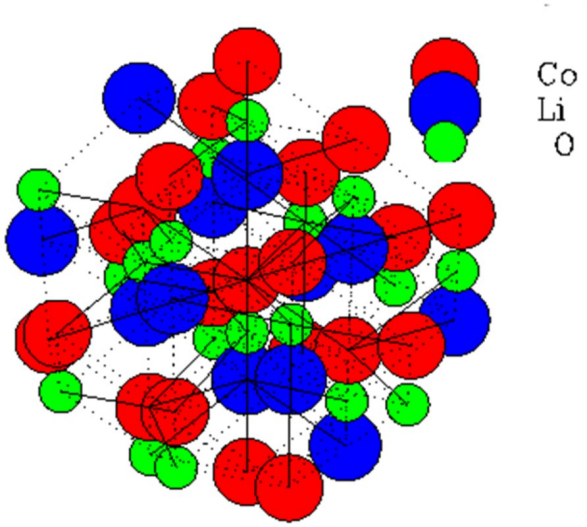

Figure 2. Crystal structure of layered $LiCoO_2$ using ref. [21]. The image was plotted using refined parameters in GNXAS software [22].

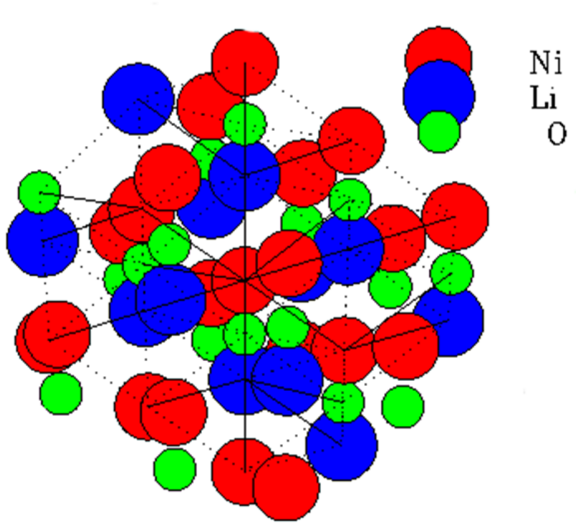

Figure 3. Crystal structure of layered $LiNiO_2$ using ref. [32]. The image was plotted using refined parameters in GNXAS software [22].

membrane that allows the electrolyte to diffuse in, avoids the short circuiting between the two electrodes and allows the ions to move through it. The electrolyte should be ionically conducting and electronically insulating in principle, however, the actual properties of the electrolyte are more complicated [3].

The improved performance of the LIBs battery depends on the material of the components used in the battery [3-6]. $LiCoO_2$ is found reasonably thermally and chemically stable and environmental friendly. However, there are associated challenges as well, such as its low conductivity and reversible capacity [7-10]. Also, Co is less available and expansive as compared other transition metals such as Mn, Ni and Fe. In addition, $LiCoO_2$ based battery undergoes severe degradation when overcharged – better competitors could be suggested – much of the current research in the field is focused to overcome these drawbacks [11-13]. The major development in rechargeable lithium batteries was made when $LiCoO_2$ was replaced with $LiCo_{1-x}Ni_xO_2$ as the cathode material, leading to considerably enhanced conductivity and reversible capacity. This generated a surge of exploiting other transition metals in LIBs – stringent structural stability challenges have been addressed, which occur especially during the charging process, when most of the lithium is removed from the cathode. We can now distinguish between these materials based on their structural properties, that is, layered structure (generally based Co and Ni oxides), spinel structure (Mn oxide based) and olivine structure (Fe phosphates based) which is a relatively new system and is considered to have various advantages over its other counterparts.

In this review, we shall give brief description of structural properties of layered and spinel systems and then olivine system in somewhat more detail. Comparison will be made between the olivine $LiFePO_4$ and other cathode systems used in the last decade. A detail on the recent work including the carbon coated composite material of $LiFePO_4$, their electrochemical and structural applications is also discussed. The structural, conductivity, capacity and performance parameters of $LiFePO_4$ cathode material will be discussed.

2. EXPERIMENTALS

Layered materials as cathodes in Li-ion batteries

In rechargeable Li-ion batteries, cathode materials are one of the key components affecting the final performance of the batteries. Among the various materials developed to act as cathodes in those cells, layered oxides are certainly very important. Layered oxide cathode materials, with a general formula $LiMO_2$ (where M=transition metal element such Co, Ni and Mn etc.) crystallize into a structure schematically depicted in Figs. 2 and 3. In these figures the oxide ions form a cubic-close-packed array with close-packed (111) octahedral site planes (rock-salt like structure). Li and

Table 1. Types of cathode materials for Lithium ion batteries (LIBS) [5, 15-19].

Cathode materials	Voltage (V) V	Charge V limit	Charge/discharge C-rates	Energy density Wh/kg	Applications
$LiCoO_2$	3.60 V	4.20 V	1C limit	110-190	Cell phone, cameras, laptops
$LiMnO_2$	3.7-3.80V	4.20 V	10C - 40C pulse	110-120	Power tools, medical equipment
$LiNiO_2$	3.70V	4.10 V	~ 5C -30C pulse	95-130	Power tools, medical equipment
$LiFePO_4$	3.2-3.30V	3.60 V	35 C cont.	95-140	Power tools, medical equipment

M ions occupy the octahedral sites [14]. This structure can be described as a layered structure corresponding to the space group $R^{-}3m$ and unit cell parameters conveniently defined in terms of the hexagonal setting. Table 1 shows the comparisons of layered and non layered cathode materials, clearly suggesting that $LiFePO_4$ is better than all the other cathodes materials.

2.1. $LiCoO_2$

$LiCoO_2$ is the most commonly used cathode material in LIBs [15,16], as it exhibits high specific capacity (274 mAh g^{-1}), low self-discharge [15] and excellent life-cycle [16]. $LiCoO_2$ forms the α-$NaFeO_2$ structure which is rock-salt lattice where the cations order in alternating (1 1 1) planes. This ion ordering results in a trigonal structure ($R^{-}3m$) and forms $LiCoO_2$ planes of lithium ions, through which lithiation and delithiation can occur [20,21]. Figure 2 shows the unit cell structure of the first neighboring distances of $LiCoO_2$ by using the Gnxas program [22] where lattice parameters are taken from et al. [21].

The cell capacity of $LiCoO_2$ LIBs increases when charging voltage increases. However, a rapid decrease in capacity is observed as the cell is cycled during recharging over the time. Several reasons have been suggested for this degradation. One is that cobalt is dissolved in the electrolyte when the electrode is delithiated during charging (deintercalation) such that complete lithianation does not occur during discharge process (intercalation) [23]. Another reason is formation of CoO_2 layer after full delithiation that also leads to the deformation of the electrode surface resulting in less capacity for lithium intercalation over the time [24]. Notice that there is a sharp change in lattice parameters as a function of lithium content [25], calling for heat treatment to obtain stoichiometric $LiCoO_2$. Therefore, a control of the surface phase content is suggest for the improve performance of cell during cycling [25]. Zou et al reported that a small amount of foreign elements can serve the purpose and gives stable cycling performances due to a suppression of the phase transformation at 4.2 V during intercalation/deintercalation process (cut-off voltage higher than 4.5 V) [26,27]. Nowadays, Mg doped $LiCoO_2$ is used for commercial Li-ion batteries. It has been found that the cycle ability of the cathode material could be improved significantly by modifying its surface with metal oxides such as Al_2O_3 and ZrO_2 [28]. However, as previously mentioned, the task of cost reduction could not be achieved because such tailoring was not meant to do so – only performance parameters were the quests for these studies.

2.2. $LiNiO_2$

Another well-know member of the $LiMO_2$ family of layered cathode materials is $LiNiO_2$, which also has the same α-$NaFeO_2$ structure as $LiCoO_2$, see Figure 3. The shown unit cell structure of the first neighboring distances of $LiNiO_2$ was drawn using the Gnxas program and lattice parameters are taken from et al [46]. $LiNiO_2$ was studied to obtain better performance and the low cost LIBs [46]. Its working voltage is more than 3.7 V and theoretical capacity is 275 mAh $g^{-}1$. $LiNiO_2$ provides important advantages such as less toxicity, lower price and higher reversible capacity as compare to $LiCoO_2$. On the other hand, it is less stable [29,30] and less ordered as compared to $LiCoO_2$. The lower degree of ordering results in nickel ions to occupy sites in the lithium plane. These hinder lithiation/delithiation also creates challenges in obtaining the appropriate composition. A small amount of doping of cobalt to $LiNO_2$ increases the degree of ordering. This leads to nickel ions to occupy sites in the nickel/cobalt plane rather than in the lithium plane. Thus $LiNi_{1-x}Co_xO_2$ has been used to take advantage of the low cost and higher capacity of nickel relative to cobalt [31]. Small amount of Mg doping causes strong increase in the electronic conductivity and slight decrease in the capacity. R. Sathiyamoorthi et al., has synthesized the Mg doped $LiNiO_2$ by low temperature solid state reaction. The Mg doped $LiNiO_2$ is single phase and stable.

With the increase of Mg concentration the peak gets broaden, which shows small crystalline size. Enhanced reversibility of the Li intercalation/de-intercalation reaction is obtained. Charged/discharged studies showed the batter capacity retention and cycleability of Mg doped $LiNiO_2$. And it shows the high performance for Li-ion cells [33] B.V.R. Chowdari et al., synthesized solid state reaction. Improve the cyclic behavior and performance of the cell [34] Small amount of Co doping in $LiNi_{1-x}Co_xxO_2$ helps to reduce the amount of nickel in the lithium layer and have been shown to improve capacity. Increased cobalt content can also reduce the loss in capacity during cycling. The improved performance has been attributed to cobalt, which increases the conductivity and improves the structural stability of the cathode. Although nickel in the lithium layer can be detrimental to lithium transport, it

Table 2. Comparison of layered structure and variation w. r. t. doped material in electrochemical and structural properties.

Cathode materials	Synthesis method	Electrochemical properties	Structural properties	Dopant
$LiCoO_2$	Solid-state method [42].Thoroughly mixing of stoichiometric amounts of different materials under Ar atmosphere at 550 ^{0}C [41].Citrate precursor method	Stable high capacities over 30 charge / discharge. Fading at 165-170 mAh/g when doped with Cu and Zn. Improved capacity retention. Cyclic stability.	Poor cycleability with increase of Li. Phase change [41]. Stable. Single phase	Mn, Cu, Fe, and Zn Mg [41, 43]. Mg
$LiNiO_2$	Conventional solid state reaction low temperature Solid state reaction	Lower capacity. Improved cyclic behavior. Improved capacity retention, cycleability and better cell performance. irreversible capacity	Phase transitions. Increase in thermal stability. Single phase and stable.	Co, Ti
$LiMnO_2$	Co-precipitation and freeze-drying route. Solid state reaction.	Al, Mn doping improves the capacity fading. Improved capacity retention and rate capability.	Phase change and disorderedness in the structures.	Al, Mn, F and Li

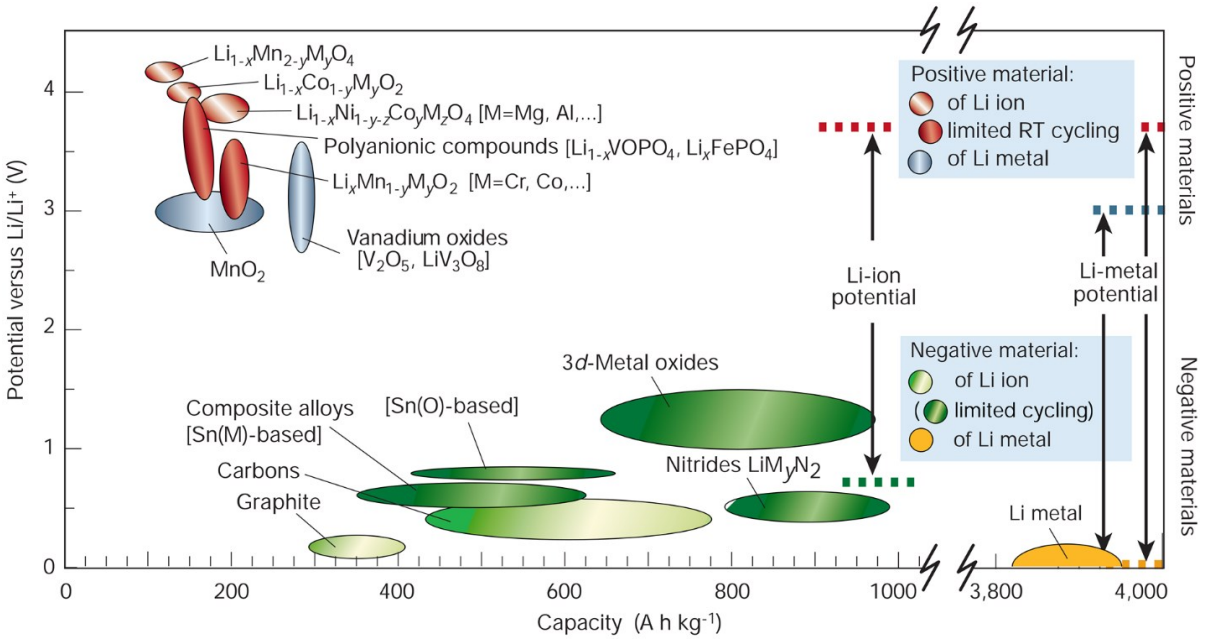

Figure 4. Voltage versus capacity for positive and negative electrode materials. The pictorial view represents presently used and next generation of rechargeable Li-based cells. The output voltage values for Li ion cells or Li metal cells are remarkably high as compared with their counterparts. Notice that there is a huge difference in capacity between Li metal based systems and the other negative electrodes, which is why there is still great interest in solving the problem of dendrite growth [38].

is shown to stabilize the structure during delithiation and improve cycling performance [15, 33].

So that is why Co is replaced with Ni. Table 2 shows the comparison of all three cathode materials and how doping effect their electrochemical and structural properties.

2.3. $LiMnO_2$

$LiMnO_2$ compounds have become of most interest as intercalation electrodes for rechargeable lithium batteries because of their high theoretical capacity 285 mAh^{-1} and low cost compared to $LiCoO_2$. $LiMnO_2$ forms a monoclinic structure which has the same cation ordering of the α-$NaFeO_2$ structure [35]. The most commonly used Li (Ni, Mn, Co) O_2 composition contains equal amount of these three transition metals: Li $(Ni_{1/3}Mn_{1/3}Co_{1/3})O_2$. This material has good rate capability, high capacity and can operate at high voltage. During cycling, the capacity of the cell leads to rapid loss while increase in voltage [30] Yet-Ming Chiang et al., synthesized Al, Mn doped $LiMnO_2$ by using the Co-precipitation and freeze-drying route [36] Al and Mn doping improves the capacity retention of the $LiMnO_2$ battery. It was also observed that the phase change and disorderness occured in the structure [36] T.J. Kim et al. synthesized the $LiMnO_2$ by using solid state route. The fluorine modified $LiMnO_2$ cathode exhibits improved capacity retention and rate capability [37].

2.4. Non-layered cathodes

Non-layered materials have also been the subject of intensive research. Guyomard and Tarascon worked at the Bell Communications Research Laboratory gave new motivation to the development

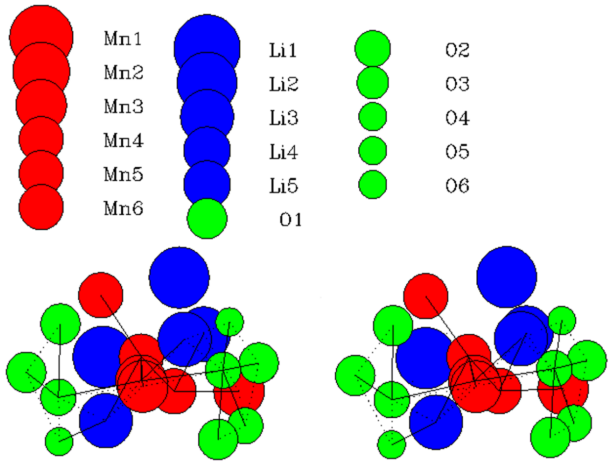

Figure 5. Crystal structure of $LiMn_2O_4$ using ref. [22, 48]. The image was plotted using refined parameters in GNXAS software.

of rocking-chair batteries by using graphite carbon as anode and $LiMn_2O_4$ as cathode. Lithium manganese spinel oxide and the Olivine $LiFePO_4$ are the most promising candidates up to now. These materials have interesting electrochemical reactions in 3-4 V region which can be useful when combined with a negative electrode of potential sufficiently close to lithium. The present performance of some electrode materials presently under consideration for Li-ion cells is summarized in Fig. 4. [38]. Recently, 5 V materials have emerged as a different option. They also include selected spinel

oxides and Olivine related solids. These alternative materials increase the working potential sufficiently to provide acceptable cell voltages when combined with a negative electrode working significantly above 0 V versus lithium. The combination of 5 V electrodes with an appropriate anode can be considered to be a third generation of lithium-ion batteries, having high power density and avoiding electro deposition of lithium at the anode. Here we will briefly describe the main features of $LiMn_2O_4$ and Olivines.

2.5. Spinel $LiMn_2O_4$

The spinel compounds $LiM_xMn_{1-x}O_4$ (M = Metal element) are attractive cathode materials for replacing Co and Ni based layered cathode materials of Li-ion batteries [39]. In particular, they have been extensively studied as positive electrode materials of large size Li-ion batteries for power sources of hybrid electric vehicles (HEV), because they have several advantages such as lower cost, high capability and higher thermal stability, as compared to those of Co and Ni based layered materials [40, 41]. As shown in Figure 5 the unit cell structure of the 1st neighboring distances of $LiMn_2O_4$ by using the Gnxas program and lattice parameters are taken from the ref, [63]. the $LiMn_2O_4$ crystallizes in the space group $Fd3^-m$ with Li and Mn present in tetrahedral and octahedral sites within the cubic close-packed oxygen array respectively [42]. However, those spinel compounds have a lower capacity as compared to the cathode materials that form the α-$NaFeO_2$ structure described above [55]. During cycling, control of phase change occurs in $LiMn_2O_4$ cathodes and is considered to be one of the challenges [43, 44]. $LiMn_2O_4$ cathodes have been field tested in the DC power supply for an operating telecommunication transceiver. In these tests, rapid loss of capacity occurred in first few days but with the passage of time the capacity loss decreased. During charging this initial loss is due to the loss of oxygen [45, 46]. The dissolution of manganese in the electrolyte has also been observed during storage and capacity loss [46], associated with changes in crystallinity and morphology of the particles [47].

Other effects take place when other transition metals such as iron and cobalt are added to $LiMn_2O_4$ [49-52]. Discharge plateaus at high voltage were observed when adding iron in $LiMn_2O_4$, while the capacity retention improves during cycling for cobalt-doped electrodes. However, the most common doping is nickel, which has been found to decrease the electric conductivity and lattice parameters of $LiMn_2O_4$ [53]. The capacity was found to increase with increasing manganese content and a 3:1 Mn:Ni ratio (i.e.$Mn_{1.5}Ni_{0.50}O_4$) is the most commonly used composition [54]. Disordered spinel structure has been shown to have higher capacity while the manganese and nickel cations were found to be ordered on the octahedral sub-lattice [55, 56]. Addition of nickel to the surface of $LiMn_2O_4$ through coatings rather than a dopant was also found to be effective in improving capacity retention during cycling [76]. Coating of $LiMn_2O_4$ spinel with $LiCoO_2$ was observed to improve the high temperature performances with the reduction in capacity and specific energy [57]. Table 3 shows the summary of doping effects (Co, Al, Cr, Ni, Li etc) on $LiMn_2O_4$.

2.6. Olivine $LiFePO_4$

$LiFePO_4$ has recently attracted considerable attention since it was first proposed by Padhi et al. [6], because of its potential application as the next generation cathode material in LIBs. Compared with conventional cathode materials $LiCoO_2$, $LiNiO_2$, $LiMn_2O_4$ and $LiFePO_4$ has many advantages such as high theoretical capacity (ca. 170 mA h g-1) and moderate operating flat voltage (the Fe^{3+} /Fe^{2+} redox couple is conveniently located at 3.4 V versus Li^+ /Li, which is compatible with common organic, as well as polymer electrolytes) [58]. In the past decade, a number of new cathode materials have been developed as alternative cathode materials for Li-ion batteries. However, none of them are in real industrial applications so far. A group of lithium transition metal polyanion compounds, incorporating polyanions XO^{3-}_4 (X= S, P, As, Mo) has been extensively investigated as new cathode materials for Li-ion batteries [59]. Padhi first demonstrated that orthorhombic $LiFePO_4$ could be used as a cathode for rechargeable Li-ion batteries [6]. In particular, the olivine type $LiFePO_4$ (triphylite) has attracted much attention as a suitable cathode material [9, 60]. $LiFePO_4$ has been extensively studied because of its attractive properties such as inexpensiveness, non toxicity, high theoretical capacity (170$mAhg^{-1}$), excellent cycling and thermal stability [5, 8, 61, 62]. Figure 6 showed the unit cell structure of the 1st neighboring distances of $LiFePO_4$ by using the Gnxas program and lattice parameters are taken from the ref [63].

$LiFePO_4$ has an ordered Olivine structure (space group Pnma) in which Li, Fe and P atoms occupy octahedral 4a, octahedral 4c and tetrahedral 4c sites, respectively. The oxygen atoms are arranged in a slightly distorted, hexagonal close-packed arrangement. The FeO_6 octahedral shares common corners in the b-c plane and the LiO_6 octahedral form edges sharing chains in the b direction. The separation of the FeO_6 octahedral by PO_4 polyanions significantly reduces the electrical conductivity of the material [59]. The key drawbacks of $LiFePO_4$ are its low electronic conductivity and reversible capacity. Various synthesis approaches have been employed to improve the conductivity and cycle ability of the $LiFePO_4$ [9, 64-66].

3 RESULT AND DISCUSSION

Doping effect on Composite $LiFePO_4$ cathode material

Many studies have been devoted to optimize the material for better electrochemical performance and try to understand the lithium intercalation/deintercalation mechanism [67-69]. It has been shown [6, 10] that significant increase of the electrical conductivity

Table 3. Variation in structural and electrochemical properties of the spinel structure by using different dopants.

Cathode Material	Synthesis method	Electrochemical properties	Structural properties	dopants
$LiMn_2O_4$	Conventional method [60]. Solid-state reaction [64-65]. Sucrose-aided combustion method [66]. Sol–gel method [67]. spray-drying method & Tartaric acid gel method [72].	Li doping improved. Cycling performance. Improved capacity retention and Cycling performance Improve in capacity retention and cycling stability	Li doping improved the structure stability. Single Phase and stabilized spinel structure Single phase.	Li [65] Co, Li [64,65,67] Al^{3+}, $Ni^{2+,}$ Cr^{3+}, Co^3 [66] $LiNi_{0.05}Mn_{1.95}O_4$ [72]

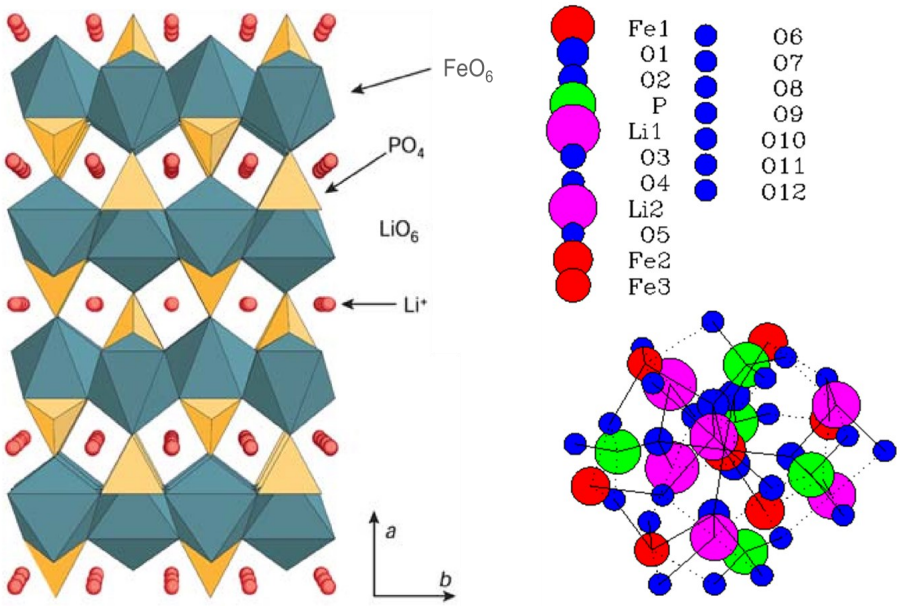

Figure 6. The crystal structure of olivine $LiFePO_4$ projected along [001] (left): FeO_6 structures are distorted octahedral and PO_4 are distorted tetrahedral. Li ions are surrounded by 6 oxygen atoms. Crystal structure of $LiFePO_4$ using ref. [22, 38] and [63](right). The structures were plotted using GNXAS software.

can be induced by controlled non stoichiometry, carbon coating and cation doping improves the performance of current electrodes. For example, olivine compounds $LiFe_{1-x}Mn_xPO_4$ were studied in order to examine the doping effect of low concentration of Mn. It was observed that Mn influence on the electrochemical performance of the olivine cathode and enhanced the initial capacity and electrical conductivity [70, 71]. It has been shown also that chlorine doping also improve the electrochemical performances [72]. A significant example for the improvement in performance obtained by controlled doping is reported by Shin et al. [73]. In his work Cr doped $LiFePO_4$/C olivine compounds synthesized by mechanochemical methods are studied in detail. The simultaneous treatment of carbon coating and Cr doping improved the rate performance of the $LiFePO_4$ batteries. It is shown in Fig. 7, that Carbon coating and Cr doping allow excellent rate performances and discharging capacity (improved up to 120 mAhg−1 at 10C rate). During cycling the structural change was also investigated. The Cr doping was found to assist the phase transformation between triphylite and heterosite during cycling and conductivity was improved by carbon coating. Liu et al. [74] synthesized the $LiFePO_4$/C composite by ball milling combined with spray- drying method.

This composite gives a high electronic conductivity with long term cyclability at a high C-rate. It also provides both the high specific energy and power required for a Li-ion battery. C.S. Sun et al., synthesized $LiFePO_4$/C and V-doped $LiFePO_4$/C cathode material by carbothermal reduction method. Figure 8 shows the CV and Charge/discharge curve of Pristine and V-doped $LiFePO_4$/C cathode materials. V-doped $LiFePO_4$/C showed a high discharge capacity at room temperature. The significantly improved high-rate charge/discharge capacity was attributed to the increased diffusion capability [75].

In V-doped $LiFePO_4$ olivine the lattice structure is not perturbed,

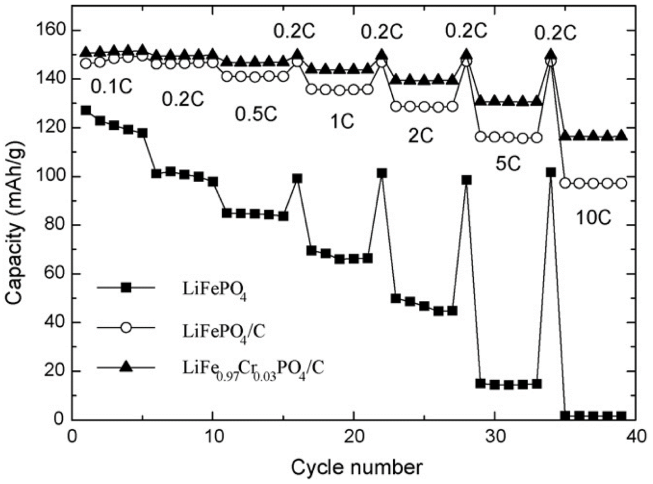

Figure 7. Rate performance of $LiFePO_4$, $LiFePO_4$/C and $LiFe_{0.97}Cr_{0.03}PO_4$/C during discharging at various rates (from 0.1to 10 C) [73].

but variations of the lattice parameter were observed as a function of doping. The XRD diffraction pattern of various V concentration and all peaks shows the olivine phase with orthorhombic ordered structure. And there was no evidence of any impurity peaks. Long-cycle performances were improved by optimizing the distribution of particles and improving the conductivity through carbon coating and V doping as shown in figure 9.

Doping of $LiFePO_4$ olivine with different ions (D=Zr, Nb, Cr) showed that the dopant resides primarily on the M1 (Li) site. The low doping level (3%) did not allow assessing a correlation be-

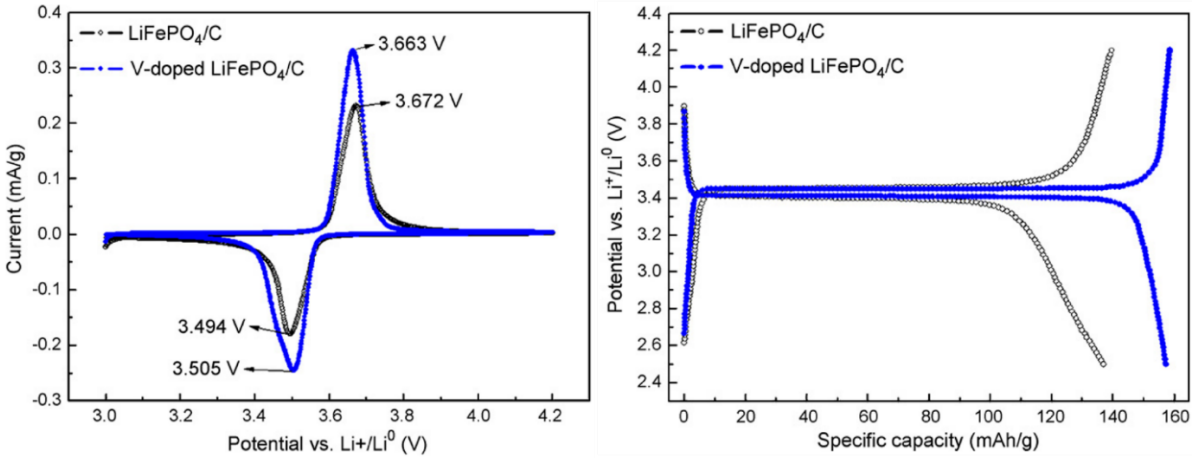

Figure 8. Cyclic voltammetry (CV) curves for pristine and V-doped $LiFePO_4/C$ measured with a scanning rate of 50 μVs^{-1}. Charge / discharge curves refer to the first cycle, measured at 0.1C (left). Potential is plotted against specific capacity for the same samples (right) [75].

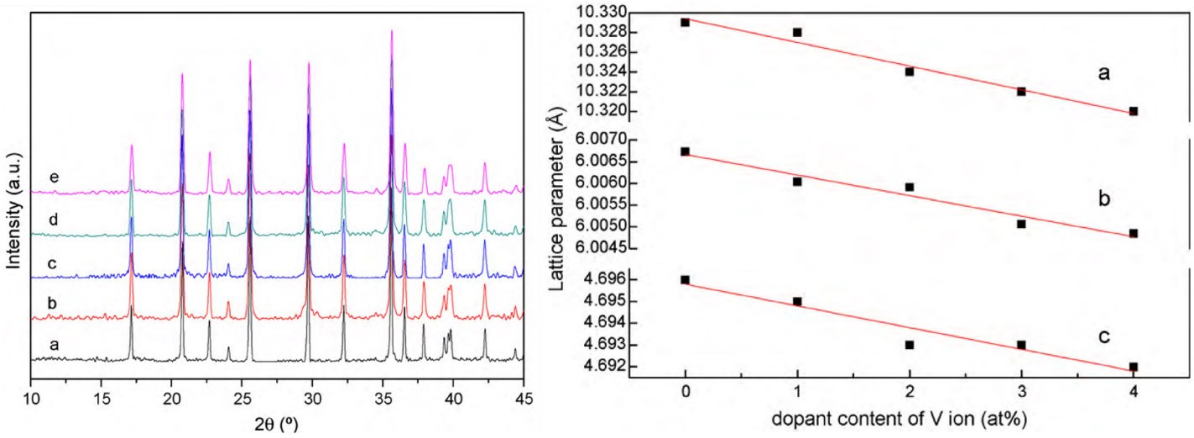

Figure 9. X-ray diffraction patterns of various V ion contention samples (left), and variation of lattice parameters with the substitution degree [61].

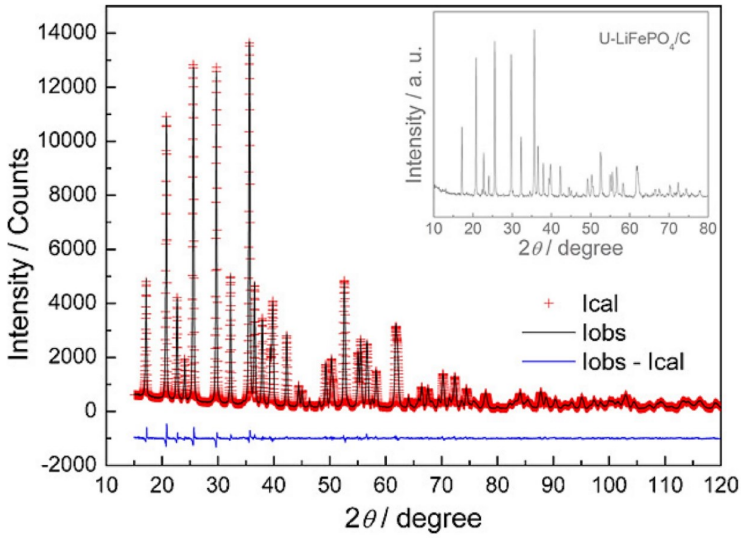

Figure 10. Rietveld profile refinement of XRD patterns for M-$LiFePO_4/C$ powders (Rwp = 0.0876, Rp = 0.0688). The inset shows XRD pattern of U-$LiFePO_4/C$ [79].

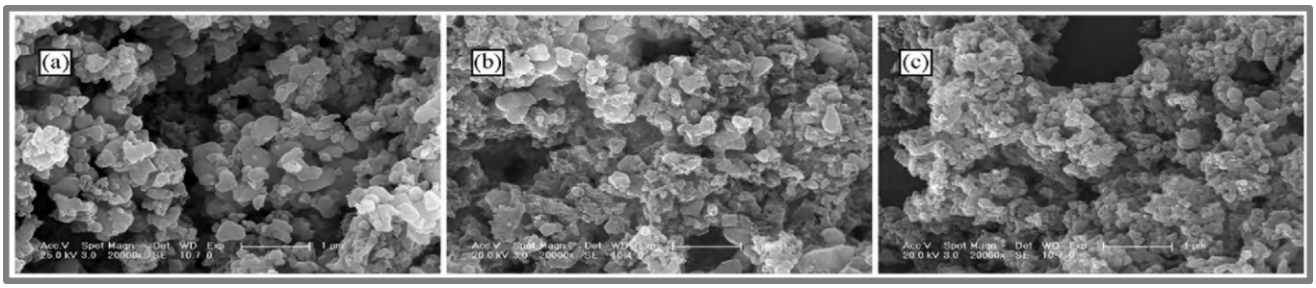

Figure 11. SEM images of pure $LiFePO_4$ (a), $LiFePO_4$/C (b) and Ni doped $LiFePO_4$/C (c) [81].

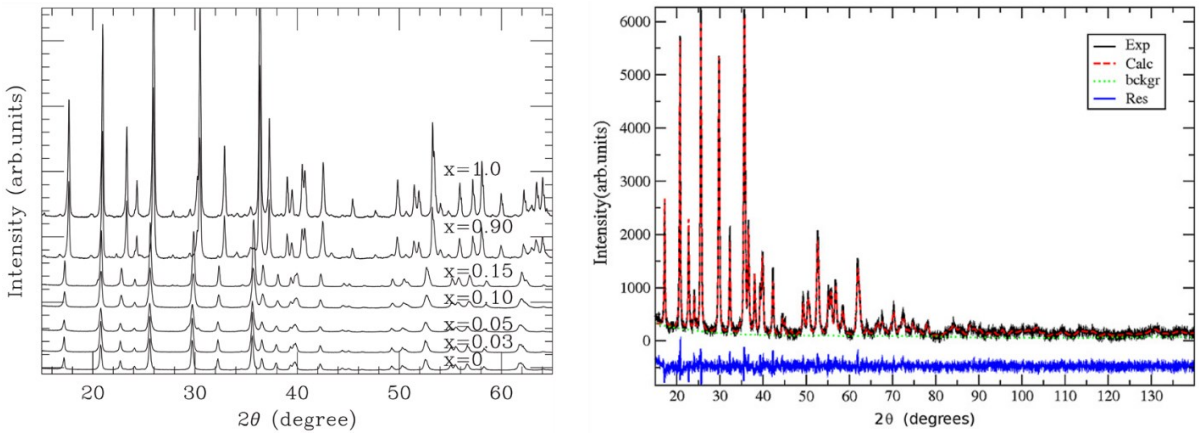

Figure 12. X-ray diffraction patterns of the $LiFe_{1-x}Ni_xPO_4$ solid solutions obtained for different doping fractions *x* (left). Example of an XRD Rietveld refinement of the powder XRD pattern in the whole angular range ($LiFe_{1-x}Ni_xPO_4$, x = 0.1) (right). Several curves are shown: experimental data (Exp, solid black line), calculated pattern (Calc, dashed red line), background (back, dotted green), and residual curve (Res, solid blue line) [9].

tween the dopants and improvement of the conductivity. On the other hand, the size of Li channels was found to be slightly increased (0.3 %) without influencing the Li-ion mobility [76]. Mg-doped $LiFePO_4$ showed a better rate performance [2]. Ti doped olivine $LiFePO_4$ have been synthesized by solid state reaction. To doping improved the rate capacity [77]. La-doped olivine $LiFePO_4$ cathode materials have been synthesized by solid-state method at high temperature. La doping did not affect the structure of the cathode material; improve capacity performance, cyclic stability and electronic conductivity[78]. Multi-doping with different ions was also carried out using novel synthesis routes. Multi-doped $LiFePO_4$/C composite is shown to improve the performance of the cells [79]. XRD (Rietveld-refinement) show that multidoped $LiFePO_4$/C is a single olivine phase, well crystalline with no evidence of presence of any impurity peaks (see Fig. 10 for a typical XRD pattern). XRD Rietveld refinement of the multi-doped alloy M-$LiFePO_4$/C confirms that Mn, V, and Cr atoms occupy the Fe site and do not introduce any olivine $LiFePO_4$. While the doped Li (M, Fe) PO_4 (M=La, Ce, Nd, Mn, Co, Ni) have also been synthesized by solvothermal method.

Electronic conductivity of $LiFePO_4$ is increased of the order of 1-3 by doping, but carbon coating is also needed to improve the conductivity of the cell. Among all these dopants, Nd was found to be the more effective [67, 80] In recent times, $LiMPO_4$ (M = Mn, Fe, Co, and Ni) multiwalled carbon nanotubes have been studied, showing high capacity and excellent rate capability [59]. Also Zn-doped $LiFePO_4$ increases the conductivity, discharge capacity and rate capability. Zinc doping was found to improve the reversibility, rate capability and conductivity of the cell. Zn doping was found to stabilize the crystal structure inducing a slight expansion of the lattice volume [62] Cu-Sn-based negative electrode of the Li-ion battery was found to improve the charge/discharge performance [66]. Ni-doped $LiFePO_4$/C nanocomposites were synthesized by solid state reaction method, without affecting the olivine lattice structure. XRD results have shown that all the diffraction peaks are indexed to an olivine orthorhombic crystal structure, with no evidence of presence of any impurity phase. At 0.2 C rate Ni-doped $LiFePO_4$/C nanocomposite shows a discharge capacity of 170mAhg^{-1}, which approximately coincides with the theoretical value. However this nanocomposite material shows excellent charge and discharge capability and long cyclability. At high C rate this material exhibits high capacities of 150 mAhg^{-1} and 130 mAhg^{-1}. Ni doping was found to enhance the electronic conductivity, reducing the particle size in the range of 20-60 nm [69, 81] (see also electron microscope images in Fig. 11).

L. Tabassam et al., synthesized the samples with solid solutions method. $LiFe_{1-x}Ni_xPO_4$ with x ranging from 0.0 to 0.15 and from 0.9 to 1.0 were successfully synthesized. Figure 12 shows the XRD diffraction patterns and Rietveld analysis of x=0.1% Ni doped $LiFePO_4$. The Rietveld analysis shows that the unit cell volume

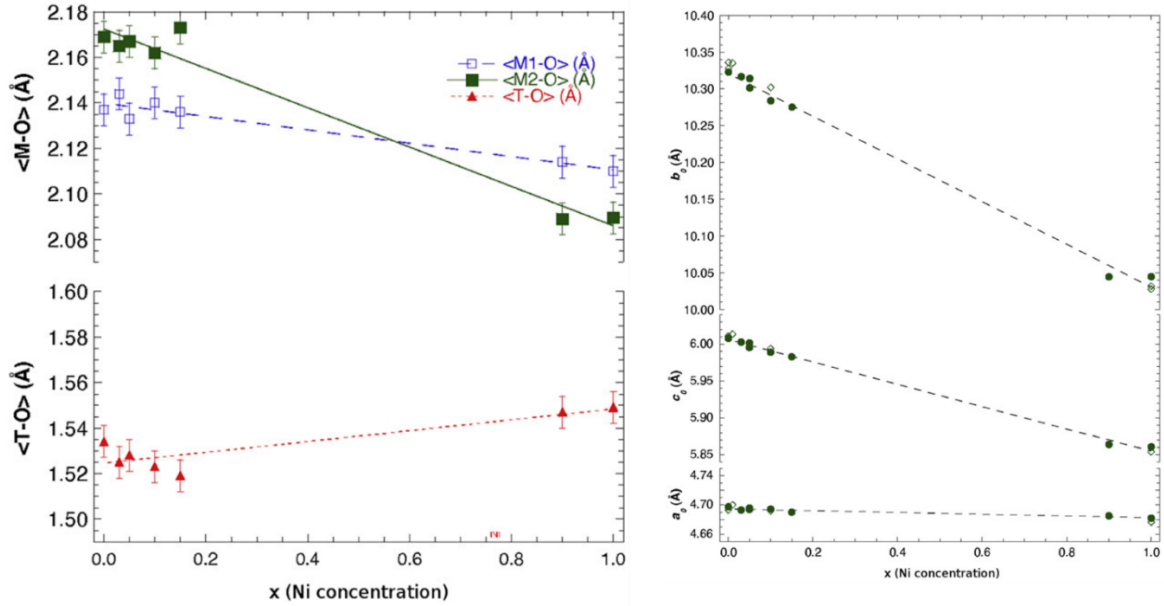

Figure 13. Average first-neighbor interatomic distances as determined by XRD Rietveld refinement, for different Ni concentrations, *x*. <MO> (metaleoxygen) average distances are reported as squares (filled or empty for M2 and M1 sites, respectively). <T-O> distances are reported as filled triangles in the lower part of the figure. Linear interpolations of those distances are shown as dashed lines. Unit cell parameters a_0, b_0, and c_0 of $LiFe_{1-x}Ni_xPO_4$, as a function of Ni concentration *x* [9].

decreases an-isotropically with increasing Ni content x.

Figure 13 shows that the average equilibrium distances <M1-O>, <M2-O> and <T-O> (where M1 and M2 are the octahedral and T is the tetrahedral site) and the average Ni-O and Fe-O inter-atomic distances [9] were obtained by XRD and XAS refinement respectively, showing that the overall linear decrease of the unit cell volume can be ascribed to the decrease of the M2 average size with increasing Ni occupancy.

XRD and XAS techniques indicate that Li occupies the M1 site, while both Fe and Ni reside mostly in the M2 site of the olivine structure. The shorter Ni-O bonding distances are found to induce a reduction of the average cell size, with an effect on the medium and long range structure. Moreover, the Ni-O octahedral sites have been found to be largely distorted, with two atoms at longer distances [9]. Figure 14 shows the Fe K-edge $k^2\chi(k)$ EXAFS signals of the $LiFe_{1-x}Ni_xPO_4$ samples for different Ni content x. $LiFePO_4$/NiP composite nanospheres with porous structures have been synthesized by spray technique. It was observed that by doping with NiP, the electric conductivity composite nanospheres improved by 3 to 4 order of magnitude as compared with pure $LiFePO_4$. $LiFePO_4$/NiP composite nanospheres with high capacity, high power and long life cycle are promising candidate for rechargeable Li-Ion batteries [82]. Fe K-edge XANES and EXAFS have been used to study the stability and the changes in the local atomic and electronic structure upon repeated cycling. The Fourier Transform of $Li_{1-x}Ni_{1/3}Co_{1/3}Mn_{1/3}O_2$ at Mn K-edge during the different charge cycle (SOC) During the charging the Mn- O distance remained unchanged [83]. The pre edge region of XANES spectrum which shows the strong shift from 1s→4p transition state and peak positions of the powdered sample provide evidence that iron is in the Fe^{2+} state (see Fig. 15).

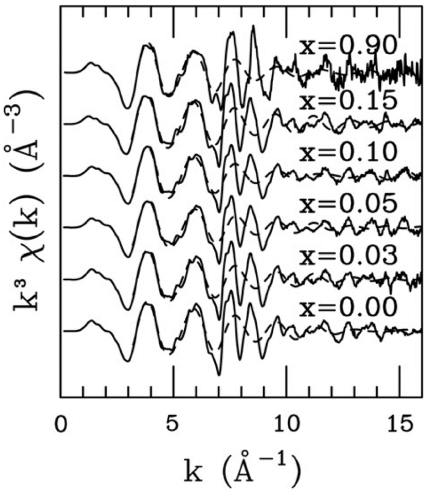

Figure 14. Fe K-edge experimental (solid lines) and calculated (dashed lines) spectra of $LiFe_{1-x}Ni_xPO_4$ samples. Only the first-neighbor component is included in the calculated signals [9].

EXAFS refinement reveals that there has been no change in the local atomic structure in the cycled $LiFePO_4$ electrodes [17, 84].

In a different study, $LiFePO_4$ was synthesized by the sol-gel technique. X-ray absorption spectroscopy (XAS) was used to investigate the local structure of lithium iron phosphate. Results of the Fe K-edge EXAFS showed that the sub microcrystalline iron phosphate material is characterized by a short range order structure

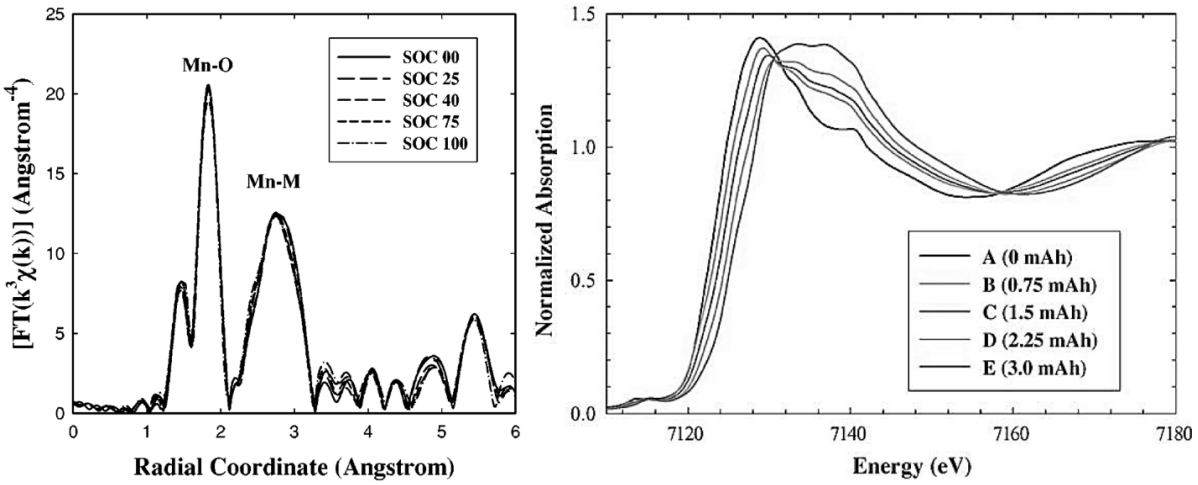

Figure 15. k3-weighted Fourier transform for $Li_{1-x}Ni_{1/3}Co_{1/3}Mn_{1/3}O_2$ at the Mn K edge at different states of charge during the charge cycle, where k range is kept 1.5–15.1 Å, M representing the transition metal atom [83](left). Data for calibrated and normalized XANES at the Fe K edge during charge. A (0 mAh), B (0.75 mAh), C (1.50 mAh), D (2.25 mAh) and E (3.0 mAh). The figure represent the different stages in the charge process at which the X-ray measurements were performed [85](right).

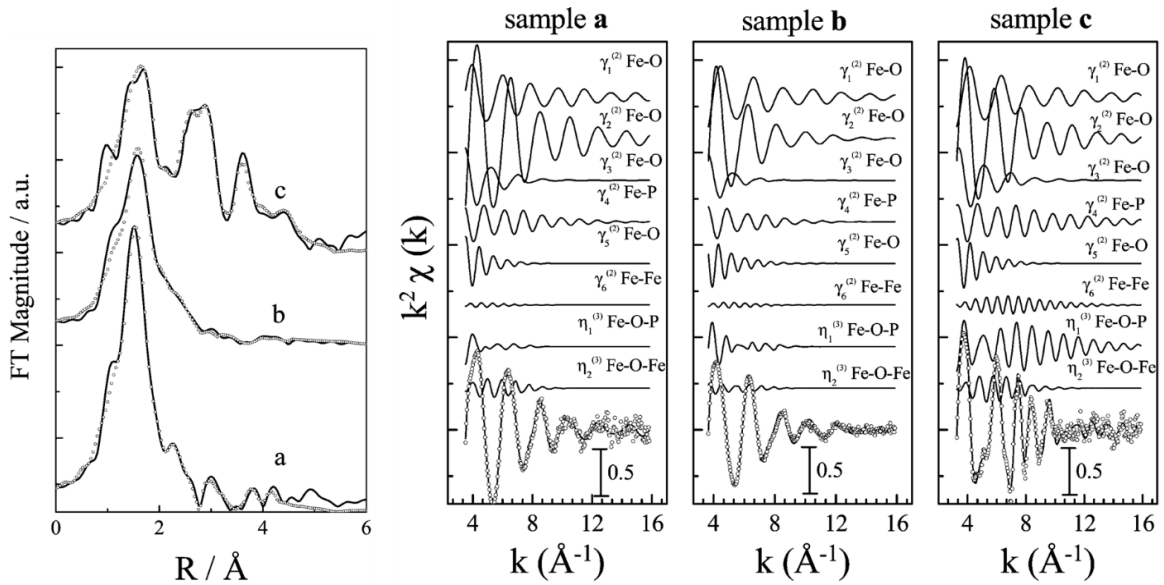

Figure 16. Experimental (dashed line) and theoretical (solid line) FT EXAFS signals of different samples obtained at the Fe K-edge (left). Details of the EXAFS analysis of the Fe K-edge of the same samples. Individual EXAFS contributions, in terms of two-body and three-body signals, to the total theoretical signal are shown. At the bottom, the comparison of the total theoretical signal (solid line) with the experimental (dots) are also [18].

slightly different from that of crystalline $LiFePO_4$. Fe-O first-shell distance increases with the heat treatment. Changes in the structure disorderness were observed during the lithiation of the amorphous precursor. In fact, Li^+ ions cause deformations on the local structure of the host upon heating, the structure becomes more organized with the Li^+ ions reaching the crystallographic sites [18] (see also Fig. 16).

Table 4 shows the doping effect of different dopants (M= Cr, Zn, V, Mn, Mo, Nb, Ti, Fe etc), and improvement in the structural and electrochemical characterization of composite $LiFePO_4$.

Arianna Moretti et al., Synthesized the V (vanadium) doped samples by using wet chemistry method. Different concentrations of V doped $LiFePO_4$ enhanced electrochemical performance which is the primary source in several morphological, structural and chemical effects with the reduction of crystallite size. The Vacancies of Li at M1 site cause the structural distortion around V and the single phase Li insertion/extraction enlarge the range of solid solution behavior. All the above factors that are responsible for

enhancing the performance of $LiFePO_4$ are related to the successful structural doping [86]. Different dopants are used to improve the structural and electrochemical performance of the batteries.

So Co was replaced with Ni. So $LiNiO_2$, which also forms the α-$NaFeO_2$ structure, is lower in cost and has a higher energy density (15% higher by volume, 20% higher by weight) but is less stable and less ordered [8] as compared to $LiCoO_2$. Another promising cathode material is $LiMn_2O_4$, which is lower in cost and safer than $LiCoO_2$. But it has lower capacity as compare to the cathode materials $LiCoO_2$ and $LiNiO_2$. Among the long list of functional materials available as storage cathodes for rechargeable Li batteries (LIB), $LiMPO_4$ (M= Fe, Ni, Co, Mn etc.).

The olivine $LiFePO_4$ (triphylite) has attracted much attention as a suitable cathode material for high-power Li-based batteries [8, 87]. $LiFePO_4$ has been extensively studied because of its attractive properties such as inexpensiveness, non toxicity, high theoretical capacity (170mAhg−1), excellent cycling and thermal stability [1, 3-6] In particular, $LiFePO_4$ is one of the most promising candidates for use of hybrid electric (HEV) and electric vehicle (EV) batteries [6]. Key factors of using these materials in batteries are their electrical and ionic (Li^+) conductivities. And the key drawbacks of $LiFePO_4$ are its low electronic conductivity and reversible capacity. Various synthesis and processing approaches have been employed to improve the conductivity and cycleability of the $LiFePO_4$ [7-9] Many studies have been devoted to optimize the material for better electrochemical performance and try to understand the lithium intercalation/ deintercalation mechanism [10, 64, 65]. The significant increase of the electrical conductivity can be induced by controlled nonstoichiometry and cation doping by improving the performance of current electrodes [6, 87]. Structural changes in triphylite due to solid solutions of a metal M with iron ($LiFe_{1-x}M_xPO_4$) may have significant effects on its solid electrolyte properties, including rates of Li diffusion and activation energies. Thus, detailed knowledge of structure in solid solutions is important in the development and design of Li-based olivine storage cathodes. Several structural studies have been performed on $LiFe_{1-x}M_xPO_4$ solid solutions [65, 67-69, 73, 82, 84]. Few of them discussed the structural variations that occur as a function of M composition x [7, 22, 81, 85, 88-92].

4. CONCLUSION

In this review article we have focused on the progress made in cathode materials in lithium ion batteries with layered and non layered cathodes. The progress is towards the high energy density, longer life cycle, good conductivity, high power density and safety characteristics of batteries. In different materials from the chemistry family; three layered and two non layered, we describe the crystal structures, ion mobilities and the stability of structures in relevance to their electrochemical properties by using different doped transition metals in the $LiFePO_4$. The results showed that the phase transformation [82] dis-orderness in the structure by using different dopants . The very important aspect is reviewed as the modification of cathode material in lithium ion batteries. Over the past decade many experimentations, characterization and design have been made for the development of the batteries with long life time. Structural characterization shows the stability and improved performance of the lithium ion batteries. In the near future we will see the improved and less costly small size batteries with long life time. Structural study of different dopants is needed to understand the enhanced performance of batteries, their life time and conductivity that can be done by analyzing the symmetric, anti-symmetric and change in type of the olivine structure. One of the major contributions is to study the nano size behavior due to the miniaturization of devices.

5. ACKNOWLEDGEMENT

This Project was funded by the National Plan for Science, Technology and Innovation (MAARIFAH), King Abdulaziz City for Science and Technology, Kingdom of Saudi Arabia, Award no. (2623).

REFERENCES

[1] Yao, J. et al., Journal of Solid State Electrochemistry, 11, 177 (2007).
[2] Hu, C. et al., Int. J. Electrochem. Sci., 5, 1457 (2010).
[3] Pollet, B.G., I. Staffell and J.L. Shang, Electrochimica Acta, 84, 235 (2012).
[4] Wakihara M., Materials Science and Engineering, R: Reports,

Table 4. Variation in structural and electrochemical properties by using different dopant in Olive $LiFePO_4$ structure.

Cathode Material	Synthesis Method	Electrochemical Properties	Structural Properties	Dopants
$LiFePO_4$	Mechanochemical process [18]. Solid-state reaction method [84]. Direct hydrothermal process. Mechanoactivation-assisted solid-state reaction [80-81]. Low-temperature solid-state method [82]. Carbothermal reduction [84-85]. Ball-milled [86]. Wet chemistry method [87]. Co-precipitation route [88]. Solid-state method [89]. Solid solution method [9] Solid-state reaction [13]. Carbothermic method [90]. Solvothermal method [91].	Excellent rate performance and conductivity improvement [18]. Improved rate capability [84]. Better life cycle and improved capacity [80-81]. Improved conductivity [82]. Higher rate capability and improved electrical conductivity [92, 76, 87]. Electrical conductivity improved [93]. Better rate performance[88] Improved capacity performance and cycling stability [89]. Improved electrochemical performance [9, 13, 90, 91]	phase transformation, Ordered structure [84]. single phase [79, 80, 83, 84, 95]. Phase change [81]. Pure phase [85, 86]. Disorderness in the structure and single phase [8, 12]. Single phase [87]. Pure phase [90].	Cr [17]. Ti [84]. Mn [80-81]. Cl [82]. V [76, 92, 87] Zr, Nb, Cr [93]. Mg [88]. La [89]. Ni [9, 13]. Multidoped LiFePO4/C [90]. Mn, Fe, Co, and Ni [91].

33, 109 (2001).
[5] Armand M. and J.-M. Tarascon, Nature, 451, 652 (2008).
[6] Padhi A.K., K. Nanjundaswamy and J. Goodenough, Journal of the electrochemical society, 144, 1188 (1997).
[7] Fan, X. et al., Nano letters, 15, 7650 (2015).
[8] Kou J., et al., ACS applied materials & interfaces, 7, 17910 (2015).
[9] Tabassam L. et al., Journal of Power Sources, 213, 287 (2012).
[10]Fergus, J.W., Journal of Power Sources, 195, 939 (2010).
[11]Belov D. and M.-H. Yang, Solid State Ionics, 179, 1816 (2008).
[12]Belov D. and M.-H. Yang, Journal of Solid State Electrochemistry, 12, 885 (2008).
[13]Doh C.-H. et al., Journal of Power Sources, 175, 881 (2008).
[14]Van Schalkwijk W. and B. Scrosati, Advances in lithium-ion batteries. 2002: Springer Science & Business Media.
[15]Antolini E., Licoo, Solid State Ionics, 170, 159 (2004).
[16]Liu H., Y. Yang and J. Zhang, Journal of Power Sources, 173, 556 (2007).
[17]Donders M. et al., Journal of the Electrochemical Society, 160, A3066 (2013).
[18]Giorgetti M. et al., Inorganic chemistry, 45, 2750 (2006).
[19]Whittingham M.S., Chemical reviews, 104, 4271 (2004).
[20]Takahashi Y., N. Kijima and J. Akimoto, Journal of Solid State Chemistry, 178, 3667 (2005).
[21]Akimoto J., Y. Gotoh and Y. Oosawa, Journal of Solid State Chemistry, 141, 298 (1998).
[22]A. Di Cicco, ed. Gnxas: A software package for advanced exafs multiple-scattering calculations and data-analysis. ed. M.M. A. Filipponi, et al., 2009, TASK Publishing, Gdansk, Poland. : Camerino, Italy.
[23]Amatucci G., J. Tarascon and L. Klein, Solid State Ionics, 83, 167 (1996).
[24]Amatucci G., J. Tarascon and L. Klein, Journal of the electrochemical society, 143, 1114 (1996).
[25]Wang Y. and G. Cao, Advanced Materials, 20, 2251 (2008).
[26]Zou M., et al., Chemistry of materials, 15, 4699 (2003).
[27]Zou, M., et al., Materials research bulletin, 40, 708 (2005).
[28]Cho J., Y.J. Kim and B. Park, Journal of the electrochemical society, 148, A1110 (2001).
[29]Tang W. et al., Energy & Environmental Science, 6, 2093 (2013).
[30]Lu Z. et al., Journal of the electrochemical society, 149, A778 (2002).
[31]Wakihara M. and O. Yamamoto, Lithium ion batteries: Fundamentals and performance. 2008: John Wiley & Sons.
[32]Gražulis S. et al., Nucleic acids research, 40, D420 (2012).
[33]Sathiyamoorthi R. et al., Journal of Power Sources, 171, 922 (2007).
[34]Chowdari B., G.S. Rao and S. Chow, Solid State Ionics, 140, 55 (2001).
[35]Jang Y.I. et al., Electrochemical and solid-state letters, 1, 13 (1998).
[36]Chiang, Y.M. et al., Electrochemical and solid-state letters, 2, 107 (1999).
[37]Kim, T.-J. et al., Journal of Power Sources, 154, 268 (2006).
[38]Tarascon J.-M. and M. Armand, Nature, 414, 359 (2001).
[39]Thackeray M. et al., Materials research bulletin, 18, 461 (1983).
[40]Takami N. et al., Journal of the electrochemical society, 156, A128 (2009).
[41]Matsushima T., Journal of Power Sources, 189, 847 (2009).
[42]Sinha N.N. and N. Munichandraiah, Journal of the Indian Institute of Science, 89, 381 (2009).
[43]Liu Q., et al., Journal of Power Sources, 173, 538 (2007).
[44]Thackeray M. et al., Journal of Power Sources, 81, 60 (1999).
[45]Deng B., H. Nakamura and M. Yoshio, Journal of Power Sources, 180, 864 (2008).
[46]Liu Y. et al., Rare Metals, 28, 322 (2009).
[47]Belharouak I. et al., Journal of the electrochemical society, 159, A1165 (2012).
[48]Tateishi K. et al., Acta Crystallographica Section E: Structure Reports Online, 60, 18 (2004).
[49]Arora P., B. Popov and R.E. White, Journal of the electrochemical society, 145, 807 (1998).
[50]Wang C. et al., Journal of Power Sources, 189, 607 (2009).
[51]Amarilla J. et al., Journal of Power Sources, 191, 591 (2009).
[52]Zhao S. et al., Journal of Alloys and Compounds, 474, 473 (2009).
[53]Ohzuku T., S. Takeda and M. Iwanaga, Journal of Power Sources, 81, 90 (1999).
[54]Patoux S. et al., Journal of Power Sources, 189, 344 (2009).
[55]Shaju K.M. and P.G. Bruce, Dalton Transactions, 40, 5471 (2008).
[56]Liu J. and A. Manthiram, Chemistry of materials, 21, 1695 (2009).
[57]Yi T.-F. et al., Ionics, 15, 779 (2009).
[58]Li Z., D. Zhang and F. Yang, Journal of materials science, 44, 2435 (2009).
[59]Armand M. et al., Nature materials, 8, 120 (2009).
[60]Kopec M. et al., Electrochimica Acta, 54, 5500 (2009).
[61]Hua N. et al., Journal of Alloys and Compounds, 503, 204 (2010).
[62]Li H. et al., Advanced Materials, 21, 4593 (2009).
[63]Jugović D. et al., Solid State Ionics, 179, 415 (2008).
[64]Bilecka I. et al., Journal of Materials Chemistry, 21, 5881 (2011).
[65]Delmas C. et al., Nature materials, 7, 665 (2008).
[66]Liu H. et al., Journal of Solid State Electrochemistry, 12, 1017 (2008).
[67]Lu Y. et al., Journal of Power Sources, 194, 786 (2009).
[68]Losey A. et al., The Canadian Mineralogist, 42, 1105 (2004).
[69]Tang P. and N. Holzwarth, Physical Review B, 68, 165107 (2003).
[70]Xu J. et al., Journal of applied electrochemistry, 40, 575 (2010).

[71]Wang Y. et al., Journal of Alloys and Compounds, 492, 675 (2010).
[72]Yang, L. et al., Journal of Solid State Electrochemistry, 13, 1541 (2009).
[73]Shin H.C. et al., Electrochimica Acta, 53, 7946 (2008).
[74]Liu J. et al., Electrochimica Acta, 54, 5656 (2009).
[75]Sun C. et al., Journal of Power Sources, 193, 841 (2009).
[76]Wagemaker M. et al., Chemistry of materials, 20, 6313 (2008).
[77]Yu Heng S. and L. Xing Quan, Chinese Chemical Letters, 17, 2006.
[78]Cho Y.-D., G.T.-K. Fey and H.-M. Kao, Journal of Solid State Electrochemistry,12, 815 (2008).
[79]Wu Z. et al., Journal of Power Sources, 195, 2888 (2010).
[80]Herle P.S. et al., Nature materials, 3, 147 (2004).
[81]Ge Y. et al., Electrochimica Acta, 55, 5886 (2010).
[82]Li, C. et al., Nano Research, 1, 242 (2008).
[83]Deb A. et al., Journal of applied physics, 97, 113523 (2005).
[84]Goriparti S. et al., Journal of Power Sources, 257, 421 (2014).
[85]Deb A. et al., Electrochimica Acta, 50, 5200 (2005).
[86]Moretti A. et al., Journal of the electrochemical society, 160, A940 (2013).
[87]Xu B. et al., Materials Science and Engineering, 73, 51 (2012).
[88]Jabbour L. et al., Cellulose, 20, 1523 (2013).
[89]Filipponi A., A. Di Cicco and C.R. Natoli, Physical Review B, 52, 15122 (1995).
[90]Filipponi A. and A. Di Cicco, Physical Review B, 52, 15135 (1995).
[91]Wilke M. et al., American Mineralogist, 86, 714 (2001).
[92]Farges, F., Physics and Chemistry of Minerals, 28, 619 (2001).